

Isotopic evidence for nitrogen exchange between autotrophic and heterotrophic tissues in variegated leaves

Cyril Abadie¹, Marlène Lamothe², Françoise Gilard² and Guillaume Tcherkez^{1*}

1. Research School of Biology, ANU College of Medicine, Biology and Environment, Australian National University, Canberra ACT 2601, Australia.

2. Plateforme Métabolisme-Métabolome, bat. 630, Université Paris-Sud, 91405 Orsay cedex, France.

*Corresponding author : Prof. Guillaume Tcherkez, Research School of Biology, ANU College of Medicine, Biology and Environment, Australian National University, Canberra ACT 2601, Australia. Tel. +61 2 6125 0381. guillaume.tcherkez@anu.edu.au

Keywords: *Pelargonium*, isotopes, labelling, N-assimilation, metabolism, variegation.

1 **Abstract** (245 words)

2 Many plant species or cultivars form variegated leaves in which blades are made of green and
3 white sectors. On the one hand, there is little photosynthetic CO₂ assimilation in white tissue
4 simply because of the lack of functional chloroplasts and thus, leaf white tissue is
5 heterotrophic and fed by photosynthates exported by leaf green tissue. On the other hand, it
6 has been previously shown that the white tissue is enriched in nitrogenous compounds, such
7 as amino acids and polyamines, which can in turn be remobilized upon nitrogen deficiency.
8 However, the origin of organic nitrogen in leaf white tissue, including the possible
9 requirement for N-reduction in leaf green tissue before export to white tissue, has never been
10 examined. Here, we took advantage of isotopic methods to investigate the source of nitrogen
11 in the white tissue. A survey of natural isotope abundance ($\delta^{15}\text{N}$) and elemental composition
12 (%N) in various variegated species shows no visible difference between white and green
13 tissues, suggesting a common N source. However, there is a tendency for N-rich white tissue
14 to be naturally ¹⁵N-enriched while in the model species *Pelargonium* × *hortorum*, white
15 sectors are naturally ¹⁵N-depleted, indicating that changes in metabolic composition and/or N-
16 partitioning may occur. Isotopic labelling with ¹⁵N-nitrate on illuminated leaf discs clearly
17 shows that the white tissue assimilates little nitrogen and thus relies on nitrate reduction and
18 metabolism in the green tissue. The N-sink represented by the white tissue is considerable,
19 accounting for nearly 50% of total assimilated nitrate.

20

21 **Introduction**

22 Many Angiosperms families have variegated species, including crops (Pringsheim and
23 Schwarz 1933). In leaf white-green variegation, there are white and green areas within the
24 same blade, sometimes forming a mottled, striped or spotted pattern. The molecular
25 mechanisms of variegation have been examined in several species (including *Arabidopsis*):
26 there is no unique cause for variegation but in most cases, the appearance of white sectors is
27 due to an alteration in chlorophyll synthesis or chloroplastic electron transport chain, thereby
28 destabilizing chlorophyll-containing complexes or causing excessive oxidative damage (for a
29 review, see Enevari 1989, Smith 1999, Yu *et al.* 2007). For example, in *Arabidopsis* mutants
30 lacking the plastidic terminal oxidase PTOX or the metalloprotease FtsH (involved in protein
31 D1 turn-over), increased photoinhibition of photosystem II and higher oxidative stress are at
32 the origin chloroplast degradation (Kato *et al.* 2009, Foudree *et al.* 2012, Putarjunan and
33 Rodermeil 2014). Also, a link with the general regulation of chloroplastic transcription has
34 been demonstrated: recently, some suppressors of variegation in *Arabidopsis* have been
35 shown to be a sigma factor (SIG6) and a chaperone-like protein (SVR4) involved in
36 chloroplastic RNA polymerase activity and nucleoid reorganization, respectively
37 (Powikrowska *et al.* 2013, Hu *et al.* 2015). In addition to obvious changes in carbon
38 metabolism (little or no photosynthesis due to the absence or alteration of the photosynthetic
39 machinery), white tissues exhibit modifications in primary nitrogen metabolism. In fact, there
40 are usually quite large amounts of nitrogenous compounds (reviewed in Tcherkez *et al.* 2012)
41 such as free amino acids, e.g., Asn. Similarly, in albino maize seedlings, higher leaf contents
42 in Asn, α -aminated compounds and ammonia have been found (Seltmann 1951). In the
43 variegated horticultural plant *Pelargonium* \times *hortorum* var. Panaché Sud, white areas have
44 been shown to be N-rich (higher elemental N content), with considerable amounts in free
45 amino acids (Tcherkez *et al.* 2012). Consistently, variegated lines of the *Arabidopsis* mutant
46 *immutans* have white sectors exhibiting a higher expression of genes associated with Asn
47 synthesis (Asp-aminotransferase and Asn synthetase) (Aluru *et al.* 2009).

48 However, the specific mechanisms by which variegation may be linked to nitrogen
49 metabolism are still rather uncertain. On the one hand, in several *Arabidopsis* mutants
50 (*immutans*, *spotty*, *var1*, and *var2*), temporary nitrogen deficiency could be the cause of an
51 increased electronic excitation pressure due to energy imbalance between photochemistry and
52 cellular utilization, thereby promoting the appearance of white sectors (Rosso *et al.* 2009). On
53 the other hand, in the mutant *immutans*, transcriptomics analyses suggest that white sectors

54 show changes nitrogen metabolism as compared to green sectors such as lower nitrate and
55 nitrite assimilation but higher Asn synthesis, and a huge change in some proteases (Aluru *et*
56 *al.* 2009). In albino mutants (chloroplast-ribosome-deficient mutants *albostrians* of barley and
57 *iojap* of maize), nitrate reductase activity is also generally 40% lower (Sawhney *et al.* 1972,
58 Borner *et al.* 1986, Borner 1986). In variegated *Chrysanthemum*, green sectors appear to be
59 enriched in transcripts associated with glutamine-oxoglutarate amino transferase (GOGAT)
60 and several other enzymes in amino acid metabolism while yellow sectors are enriched in
61 serine-glyoxylate amino transferase (Chang *et al.* 2013). Taken as a whole, it thus seems that
62 white tissues reduce nitrate to a lower extent but conversely, convert and accumulate organic
63 nitrogen in primary or secondary metabolites via intense N metabolism. Such accumulated
64 compounds can in turn be remobilized under N-deficiency to feed plant growth and
65 development (Abadie *et al.* 2015).

66 In a previous study (Tcherkez *et al.* 2012), we showed in variegated leaves of *P. ×*
67 *hortorum* the enhancement of alkaloid and Arg biosynthesis in white areas and furthermore,
68 leaf-part specific isotopic labelling (¹⁵N-nitrate solution deposited with a paintbrush)
69 demonstrated that white and green areas exchanged nitrogenous molecules (with nitrogen
70 export from green areas being quantitatively much more important). That is, ¹⁵N-nitrate
71 deposited on the green area caused a clear ¹⁵N-enrichment in the white tissue, thereby
72 suggesting that N was absorbed in green areas and subsequently translocated and metabolized
73 in white areas. However, the ¹⁵N-enrichment obtained in this study was rather low and only
74 visible with isotope ratio mass spectrometry (IRMS) on total organic matter. This was due to
75 the poor control of the absorption of the isotopic tracer when simply deposited at the leaf
76 surface. It is thus presently unknown whether ¹⁵N is transported in the form of nitrate or
77 organic N.

78 Here, we took advantage of isotopic techniques to follow the fate of N atoms between
79 leaf tissues. We first collected various samples from variegated species collected in botanic
80 gardens and public parks and greenhouses, and determined the natural isotope composition
81 ($\delta^{15}\text{N}$) using elemental analysis coupled to IRMS. We further determined both the C
82 elemental content and the natural isotope composition in ¹³C ($\delta^{13}\text{C}$) to follow the difference in
83 C metabolism between autotrophic (green) and heterotrophic (white) tissues, and to reveal
84 potential reciprocal changes in %C and %N. Since very few species have been studied to
85 disentangle metabolism in variegated leaves, we then concentrated our efforts on the model
86 species *P. × hortorum* in which considerable metabolic data has been generated previously,

87 and conducted ^{15}N -labelling (^{15}N -nitrate) on detached leaf discs in the light. Metabolomics
88 analyzes and compound-specific ^{15}N -enrichment in amino acids allowed us to quantify the
89 amount of ^{15}N incorporated in both green and white tissues when they are kept together
90 (variegated leaf discs) or not (either green or white leaf discs). Our results show that the origin
91 of nitrogen in leaf white tissue is nitrate reduction and assimilation in green tissues.

92

93 **Material and methods**

94 *Plant material*

95 The cultivar used in the present study was *Pelargonium × hortorum* var. Panaché Sud. This
96 variety is a periclinal chimera in which white areas are caused by the lack of functional
97 photosynthetic chloroplasts in both L2 (hypodermis) and L3 (mesophyll) cell layers. Plantlets
98 were generated from cuttings planted in peat for rooting and then transferred to potting mix.
99 Plants were then grown in the greenhouse under 22/18°C, 60/55% relative humidity, 16/8h
100 photoperiod (day/night). Plants were automatically watered 3 times a day with 1 g L⁻¹ nutrient
101 solution Plant-Prod 14-12-32 (Plant Prod, Puteaux, France) supplemented with 20 µL L⁻¹
102 fertoligo L (Fertil, Boulogne-Billancourt, France).

103

104 ¹⁵N-labelling

105 The procedure used is illustrated in Fig. 1. Leaf discs were collected on light-adapted plants
106 (after 6 h light in the greenhouse) and transferred to Petri dishes in a KNO₃ solution 15 mmol
107 L⁻¹ (either ¹⁴N or ¹⁵N) or distilled water. Leaf discs were sampled from either green or white
108 sectors, or just at the border so as to have half-green/half-white discs. Leaf discs were not
109 submerged (the volume of solution was adjusted to avoid submersion). K¹⁵NO₃ (31.8% ¹⁵N)
110 was purchased at Eurisotop (Saint-Aubin, France). After 4 and 6 hours in the light (300 µmol
111 m⁻² s⁻¹ PAR), discs were frozen in liquid nitrogen. Half-green/half-white discs were cut upon
112 sampling so as to separate white and green sectors and then analyse them separately.

113

114 *Metabolomic (GC-MS) analyses*

115 GC-MS analyses were done as described in Tcherkez *et al.* (2012). Briefly, gas
116 chromatography coupled to time-of-flight mass spectrometry (GC-TOF-MS) was performed
117 on a LECO Pegasus III with an Agilent 6890N GC system and an Agilent 7683 automatic
118 liquid sampler. The column was an RTX-5 w/integra-Guard (30 m x 0.25mm i.d. + 10 m
119 integrated guard column) (Restek, Evry, France). Leaf samples (20 mg of powder from
120 freeze-dried material) were ground in a mortar in liquid N₂, and then in 2 mL of methanol
121 80%, in which ribitol (100 µmol L⁻¹) was added as an internal standard. After centrifugation
122 and spin-drying, extracts were derivatized with methoxyamine (in pyridine) and N-methyl-
123 N(trimethyl-silyl)trifluoroacetamide (MSTFA). Before loading into the GC autosampler a mix
124 of a series of eight alkanes (chain lengths: C₁₀ to C₃₆) was included. Analyses were performed

125 by injecting 1 μ L in splitless mode at 230°C (injector temperature). The chromatographic
126 separation was performed in helium as a gas-carrier at 1 mL min⁻¹ in the constant flow mode
127 and using a temperature ramp ranging from 80 to 330°C between minute 2 and 18, followed
128 by 6 min at 330°C. Ionization was made by electron impact at 70eV and the MS acquisition
129 rate was 20 spectra s⁻¹ over the m/z range 80-500. Peak identity was established by
130 comparison of the fragmentation pattern with MS available databases (NIST), using a match
131 cut-off criterion of 700/1000, and by retention time using the alkane series as retention
132 standards. The integration of peaks was performed using the software LECO Pegasus.
133 Because automated peak integration was occasionally erroneous, integration was verified
134 manually for each compound in all analyses.

135

136 ¹⁵N-enrichment in amino acids

137 The compound-specific enrichment in amino acids was computed from m and $m+1$ signals
138 obtained by GC-MS (see above) on selected fragments which contained the N atom. Since the
139 $m+1$ signal also contained isotopic forms unrelated to ¹⁵N (like ¹³C, ¹⁸O, ²⁹Si, etc.) from
140 possible fragments of other unrelated, co-eluting compounds, the actual ¹⁵N content (mol ¹⁵N
141 g⁻¹ DW) was computed as the isotopic excess as follows:

$$142 \quad {}^{15}q = ({}^{15}p - {}^{14}p) \times c \times \eta$$

143 where ¹⁵ p and ¹⁴ p are the % ¹⁵N obtained using samples fed with ¹⁵N- and ¹⁴N-nitrate,
144 respectively; c is the content in the amino acid of interest (mol g⁻¹ DW); and η the mole ratio
145 of N content, i.e. moles of N per mole of amino acid (provided all N atoms are present in the
146 fragment analysed by GC-MS). ¹⁵N-percentages (¹⁵ p and ¹⁴ p) were calculated from the $m+1/m$
147 signal ratio as in Tcherkez *et al.* (2012).

148 %N and IRMS measurements

149 The elemental content and the isotope composition of organic matter (%C, %N, $\delta^{13}\text{C}$ and
150 $\delta^{15}\text{N}$) were measured using elemental analysis and mass spectrometry (Pyro-Cube coupled to
151 the IRMS Isoprime 100, Elementar, Villeurbanne, France) on samples (1 mg of leaf material)
152 weighted in tin capsules. Glutamic acid and caffeine of known isotope composition (USGS40
153 and IAEA-600, $\delta^{15}\text{N} = -4.5\text{‰}$ and $+1.0\text{‰}$ respectively, International Atomic Energy Agency,
154 Vienna, Austria) were used to calibrate isotopic analyses. Nitrogen isotope compositions $\delta^{15}\text{N}$
155 were expressed with respect to Air-N₂ (0.3677% ¹⁵N). Carbon isotope compositions $\delta^{13}\text{C}$

156 were expressed with respect to V-PDB (1.12372% ^{13}C). The apparent isotope fractionation
157 was calculated as:

$$158 \quad \Delta = (\delta_{\text{white}} - \delta_{\text{green}})/(\delta_{\text{white}} + 1)$$

159 where δ represents $\delta^{13}\text{C}$ or $\delta^{15}\text{N}$. The elemental offset (relative difference in elemental
160 composition, denoted as E) was calculated as:

$$161 \quad E = (x_{\text{white}} - x_{\text{green}})/x_{\text{green}}$$

162 where x represents the elemental content in %. The subscripts C and N denote the offset in
163 %C (E_C) and %N (E_N).

164 Samples of variegated leaves of different species and locations were collected and
165 dried in the oven at 50°C. When collected in remote regions far from the lab, samples were
166 first pressed and dried in paper envelopes and then dried in the oven. The list of sampled
167 species and locations is tabulated in Supplemental Table S1. Additional $\delta^{13}\text{C}$ and $\delta^{15}\text{N}$ values
168 associated with *Pelargonium × hortorum* obtained under N restriction are from source data in
169 Abadie *et al.* (2015).

170

171 *Statistics*

172 Statistical analysis was performed by two-way ANOVA where sample (tissue) type was
173 selected as the first factor and condition (water, nitrate) as the second factor. Differences were
174 considered to be significant when $P < 0.05$ unless otherwise stated. The multivariate
175 discriminant analysis, i.e., discrimination of samples (differentiating tissue type and
176 conditions) with metabolites was done using OPLS (orthogonal projection on latent
177 structures) carried out with Simca® (MKS Umetrics, Umeå, Sweden). The effect of each
178 metabolite in explaining the discrimination was quantified using the loading score. The
179 performance of the model generated by the OPLS-DA was quantified by the determination
180 coefficient (R^2) and the cross-validated determination coefficient (Q^2) between observed and
181 modelled Y-variable values.

182

183 **Results**

184 *Natural isotope composition in white and green tissues*

185 The relative difference in elemental content (E) and the apparent isotope fractionation (Δ)
186 between white and green tissues are shown in Fig. 2. There was little difference in either E or
187 Δ , with frequency bar charts all centred around zero (Fig. S1, Fig. 2A). The median value of
188 E_C and $^{13}\Delta$ was slightly negative, indicating lower carbon content and ^{13}C -enrichment on
189 average and accordingly, there was a positive relationship between E_C and $^{13}\Delta$ (Fig. 2B).
190 There was considerable scattering for E_N (Fig. S1C) but on average, there was no difference
191 between white and green tissues (Fig. S2). Similarly, there was on average no difference in
192 $^{15}\Delta$ (Fig. S1D, Fig. 2A). However, there was a tendency for N-rich white tissues to be ^{15}N -
193 enriched (Fig. 2C). Also, there was considerable scattering and no isotopic offset in $\delta^{13}\text{C}$ and
194 $\delta^{15}\text{N}$ values between green and white tissues (Fig. S2). By contrast, there was a visible offset
195 in δ -values in *P. × hortorum* (Fig. 3), with white tissue being on average ^{13}C -depleted by 2‰
196 and ^{15}N -depleted by 5‰. Interestingly, both plain green morphs and green areas of variegated
197 morphs were in the same range of values (Fig. 3, closed and semi-filled symbols) suggesting
198 that the isotopic difference is caused by metabolic processes associated with white tissues.

199

200 *Metabolomics pattern in white and green tissues*

201 The metabolic composition in white and green leaf tissues of *P. × hortorum* was examined by
202 GC-MS metabolomics, using leaf discs prepared in the absence or in the presence of nitrate in
203 the light (Fig. 1). 75 analytes were detected among which 66 were significantly different
204 ($P < 0.05$) between green and white tissues in a two-way ANOVA (Fig. 4A). The hierarchical
205 clustering and the heat map showed that metabolites could be sub-divided into two groups. As
206 expected, organic and amino acids and polyamine (urea, ornithine) were more abundant in
207 white tissue, and hexoses and primary N-assimilates (Glu and Gln) were more abundant in
208 green tissues, reflecting the prevalence of photosynthetic metabolism in green tissues. There
209 was nearly no effect of incubation conditions (water, nitrate), with only four metabolites
210 significantly affected (not shown on Fig. 4): β -alanine, Ile, tartarate and palmitate, all of them
211 being more abundant in the presence of nitrate compared with water. There was no metabolite
212 significant in the interaction tissue type \times condition or for the specific effect of the isotopic
213 form used (^{14}N - vs. ^{15}N -nitrate). An OPLS analysis allowed us to look more closely at
214 metabolites that best discriminated samples (Fig. 4B and C). That is, in the supervised
215 multivariate analysis, we differentiated samples into four types using 'greenness' as a

216 qualitative variable, i.e., in that order: plain white discs, white part of variegated discs, green
217 part of variegated discs, plain green discs. The statistical model generated was fully
218 satisfactory, with a general determination value (R^2) of 0.98 and a very good robustness with
219 a cross-validated determination value (Q^2) of 0.96. Sample types were thus well differentiated
220 along axis 1 (Fig. 4B), which was best determined by hexoses and hexose derivatives (right
221 hand side, Fig. 4C) and many compounds among which γ -aminobutyrate (GABA) and Tyr
222 had the highest weight (left hand side, Fig. 4C). Experimental conditions (water vs. nitrate)
223 were differentiated along axis 2 (Fig. 4B), with polyols (mannitol and sorbitol) being more
224 abundant in water and tartarate more abundant with nitrate (top and bottom of Fig. 4C,
225 respectively).

226 *¹⁵N-labelling in amino acids*

227 The isotopic enrichment in amino acids was investigated to follow the fate of ¹⁵N atoms
228 provided by labelled nitrate (Fig. 5). There was a very clear ¹⁵N-labelling in several amino
229 acids while Asn, Gly, Leu, Ile, Met, Tyr and Val represented a very small ¹⁵N-content (Fig.
230 5A). Most of the ¹⁵N was allocated to Ala, Asp, Glu and Ser (rather variable in Gln)
231 regardless of the tissue considered. However, plain white discs appeared to have much less
232 ¹⁵N (Fig. 5A, pink bars). Taken as a whole, the total ¹⁵N amount found was effectively and
233 significantly lower (about one fifth) compared with other tissues (Fig. 5B). It is worth noting
234 that white tissues that remained attached to green tissue in variegated discs behaved similarly
235 to other green tissues (Ala, Asp, Glu, Ser and total ¹⁵N). When plotted against each other (Fig.
236 6), the ¹⁵N-content in green and white tissue of variegated discs was very similar (aligned
237 along the 1:1 relationship) while plain white discs show very little ¹⁵N-build-up (slope of
238 0.14) as compared with green plain discs. In other words, this indicates that white tissues
239 alone were unable to assimilate nitrates to a high extent: the value of the slope suggests that
240 86% of the nitrogen in white tissues was inherited from green tissues.

241

242 **Discussion**

243 *Nitrogen in white tissues originates from N assimilated in green tissues*

244 The botanical survey indicates little difference in the $\delta^{15}\text{N}$ value between green and white
245 areas, suggesting that nitrogen has a common origin in both sectors (Fig. 2). There was,
246 however, considerable variation in both %N and $\delta^{15}\text{N}$ values suggesting that depending on
247 species and conditions, N allocation and metabolism may change and impact nitrogenous
248 compounds in white tissues. The loose relationship between E_{N} and the $^{14}\text{N}/^{15}\text{N}$ fractionation
249 (Fig. 2C) suggested that higher %N was associated with the accumulation of ^{15}N -enriched
250 nitrogenous molecules. However, in our model species *P. × hortorum*, there was a ^{15}N -
251 depletion of a few per mil in white tissues as compared with green tissues (Fig. 3). Such a
252 difference was unlikely to come from a lower content in nitrates, which are known to be
253 naturally ^{15}N -enriched (Gauthier *et al.* 2013): in fact, nitrates represented a very small fraction
254 of leaf N under our growth conditions, in both green and white tissues (Abadie *et al.* 2015). It
255 is thus more likely that the metabolic composition and/or specific $^{14}\text{N}/^{15}\text{N}$ isotope effects were
256 at the origin of the $\delta^{15}\text{N}$ difference. White tissues contained more polyamines, several amino
257 acids such as Ala, Asn, Val and Arg (up to 100-fold more) and simple alkaloids like tyramine
258 (Fig. 4). These compounds are downstream in N-metabolism and thus likely to be ^{15}N -
259 depleted compared to source N-assimilates Glu and Gln because of enzymatic isotope effects
260 (Werner and Schmidt 2002). Also, Ser (which appears to be transferred from green to white
261 tissues, see also below) is naturally ^{15}N -depleted due to the isotope effect in photorespiration
262 (Tcherkez 2011, Gauthier *et al.* 2013). The small ^{13}C -depletion in white tissues has been
263 suggested to come from refixation of respired CO_2 (Tcherkez *et al.* 2011). The positive
264 relationship between E_{C} and the $^{12}\text{C}/^{13}\text{C}$ fractionation (Fig. 2B) suggest that in general, the
265 higher %C was associated with the prevalence of ^{13}C -depleted molecules. In addition to
266 refixation, a change in the balance between lipids (^{13}C -depleted) and sugars (^{13}C -enriched)
267 could be involved.

268 The present results obtained with ^{15}N -labelling also indicate that white tissues
269 assimilated little nitrate alone while they incorporated ^{15}N when kept attached to green tissue
270 (Fig. 5). Interestingly, total ^{15}N -amount found in white tissues expressed in $\mu\text{mol g}^{-1}$ DW was
271 similar in white and green tissues from both plain and variegated discs (Fig. 5B and 6),
272 suggesting that 50% of ^{15}N atoms assimilated by green tissues were actually exported to white
273 tissues. In other words, when normalized to the green surface area, ^{15}N -assimilation by green
274 tissues seems to have been increased by the presence of the white tissue. Taking into account

275 the labelling time duration, the rate of ^{15}N -incorporation in plain green discs can be computed
276 to be about $8.6 \text{ nmol m}^{-2} \text{ s}^{-1}$, meaning a total nitrate assimilation into amino acids of $8.6/0.318$
277 $\approx 0.03 \text{ } \mu\text{mol NO}_3^- \text{ green m}^{-2} \text{ s}^{-1}$ (where 31.8% is the % ^{15}N in utilized nitrate) while it would
278 be about the double ($0.06 \text{ } \mu\text{mol NO}_3^- \text{ green m}^{-2} \text{ s}^{-1}$) in variegated discs. This order of
279 magnitude falls within known rates of nitrate assimilation in the light (Urbanczyk-Wochniak
280 and Fernie 2005, Tcherkez and Hodges 2008). However, the “nitrogen sink” effect described
281 above would require further examination.

282 The major products of ^{15}N -incorporation were found to be Ala, Asp, Glu and Ser (Fig.
283 5). The isotopic enrichment in Gln appeared to be more variable. The nature of the transport
284 molecule used to carry ^{15}N from green to white areas is presently uncertain. Asn is known to
285 be a common nitrogenous compound exported from leaves (for a review, see Gaufichon *et al.*
286 2012). However, Asn appeared to represent a rather small ^{15}N pool. With the data in hand, the
287 involvement of the major ^{15}N -metabolite, Glu, seems to us more likely. However, the use of
288 ^{13}C natural abundance showed that in white tissues, Ser was ^{13}C -enriched, thus having a
289 typical photorespiratory isotopic signature and suggesting that it was also exchanged between
290 green and white tissues (Tcherkez *et al.* 2011). Previous metabolomics data suggested that
291 Ser, Arg and urea metabolism could be of importance in white tissues due to relatively high
292 Ser-to-Gly ratios, very high Arg concentration and large urea-to-Glu ratios (Tcherkez *et al.*
293 2012). Here, we did not detect significant ^{15}N -enrichment in Arg and urea indicating that they
294 represent downstream metabolites synthesized from N-assimilates imported by white tissues.

295 *Functional significance of N-metabolism in white tissues*

296 The strong dependence of white tissues on green tissues to reduce and assimilate N onto
297 organic skeletons comes as no surprise, since white and albino leaf sectors are known to have
298 both a lower nitrate reductase activity (see *Introduction*) and a higher N-requirement to form
299 leaf matter (in *Pelargonium*, it is about 40% higher, Abadie *et al.* 2015) – due to a higher
300 content in many nitrogenous compounds. Having said that, such a higher N content was not
301 found consistently in all variegated species examined here (Fig. S1 and 2). In an attempt to
302 find typical patterns, we tested whether there was a significant effect of geographical origin,
303 growth N or light conditions, but no significant effect was found (not shown). It has been
304 shown in detached barley (*Hordeum vulgare*) leaf discs that exogenously added polyamines
305 (putrescine, spermine, spermidine) can prevent chlorophyll loss and apparent variegation
306 despite an accelerated proteolysis (Cohen *et al.* 1979) and in *Arabidopsis*, mutations in genes

307 known to cause a pale virescent phenotype have been shown to suppress leaf variegation in
308 *thf1* (which plays a role in down-regulating chlorophyll degradation and protection against
309 oxidative stress) (Hu *et al.* 2015). Thus it is plausible that imbalance in nitrogen allocation to
310 chlorophyll and proteins (and other nitrogenous compounds) synthesis could be linked to
311 variegation. It is likely that N metabolism of white tissues is also influenced by both growth
312 conditions as well as the type of secondary and/or primary metabolites naturally accumulated
313 in the species considered. In the case of *P. × hortorum*, leaf-accumulated compounds are
314 mostly organic acids (tartarate) and nitrogenous compounds, such as Arg and alkaloids
315 (tyramine, tryptamine and the defense compound elaeocarpidine) (Tcherkez *et al.* 2012).

316 Data on North American species show a strong association of variegated leaves with
317 the herbaceous habit in forest understories, with variegation most common in evergreen
318 leaves on poor soils (where losses to herbivores would be costly to replace) and secondarily
319 most common in spring ephemerals and spring phases of early summer species (where losses
320 to herbivores might be high due to their high leaf N content) (Givnish 1990). Under the
321 assumption that leaf variegation represents an adaptive trait to camouflage the plant against
322 color-blind herbivores (Givnish 1990), avoiding herbivory is beneficial since it avoids a
323 nitrogen cost. Such a strategy would be even more efficient if nitrogen is mostly present in
324 white sectors that are less likely to be seen and consumed by herbivores. A role of variegation
325 against herbivores has effectively been suggested several times (for a recent review, see Lev-
326 Yadun 2015). Observations and experimental data supporting this view have been provided
327 by Campitelli *et al.* (2008) for the camouflage hypothesis and by Smith (1986) and Lev-
328 Yadun (2014) for the hypothesized defensive value of mottled leaves against leaf miners. A
329 presumed role in photoprotective mechanisms has been invalidated (Esteban *et al.* 2008). Our
330 previous study has demonstrated a benefit of variegation under N-restriction in *P. × hortorum*
331 (Abadie *et al.* 2015) but the question of whether this can be generalized to other species is
332 unknown. Future studies are warranted to examine these aspects on a wider scale.

333 **Acknowledgements**

334 The authors acknowledge the financial support of the Agence Nationale de la Recherche,
335 through a Jeunes Chercheurs project, under contract JC12-0001-01, and the Australian
336 Research Council through a Future Fellowship grant, under contract FT140100645. The
337 authors also thank Edouard Boex-Fontvieille for collecting samples of variegated leaves in La
338 Martinique.

References

- Abadie C, Lamothe M, Mauve C, Gilard F, Tcherkez G (2015) Leaf green-white variegation is advantageous under N deprivation in *Pelargonium × hortorum*. *Funct Plant Biol* 42, 543–551.
- Aluru MR, Zola J, Foudree A, Rodermel SR (2009) Chloroplast photooxidation-induced transcriptome reprogramming in *Arabidopsis* immutans white leaf sectors. *Plant Physiol* 150, 904–923.
- Borner T (1986) Chloroplast control of nuclear gene function. *Endocytobiosis and Cell Research* 3, 265–274.
- Borner T, Mandel RR, Schiemann J (1986) Nitrate reductase is not accumulated in chloroplast-ribosome-deficient mutants of higher plants. *Planta* 169, 202–207. doi:10.1007/BF00392315
- Campitelli BE, Stehlik I, Stinchcombe JR (2008) Leaf variegation is associated with reduced herbivore damage in *Hydrophyllum virginianum*. *Botany* 86(3): 306–313.
- Chang Q, Chen S, Chen Y, Deng Y, Chen F, Zhang F, Wang S (2013) Anatomical and physiological differences and differentially expressed genes between the green and yellow leaf tissue in a variegated *Chrysanthemum* variety. *Mol Biotechnol* 54, 393–411.
- Cohen AS, Popovic RB, Zalik S (1979) Effects of polyamines on chlorophyll and protein content, photochemical activity and chloroplast ultrastructure of barley leaf discs during senescence. *Plant Physiol* 64, 717–720.
- Enevari M (1989) The history of research on white-green variegated plants. *Bot Rev* 55, 106–139.
- Esteban R, Fernandez-Marin B, Becerril JM, Garcia-Plazaola JI (2008) Photoprotective implications of leaf variegation in *E. dens-canis* L. and *P. officinalis* L. *J Plant Physiol* 165, 1255–1263.
- Foudree A, Putarjunan A, Kambakam S, Nolan T, Fussell J, Pogorelko G, Rodermel S (2012) The mechanism of variegation in immutans provides insight into chloroplast biogenesis. *Frontiers Plant Sci* 3, no. 260
- Gaufichon L, Masclaux-Daubresse C, Tcherkez G, Reisdorf-Cren M, Sakakibara Y, Hase T, Clément G, Avice JC, Granjean O, Marmagne A, Boutet-Mercey S, Azzopardi M, Soulay F, Suzuki A (2012) *Arabidopsis thaliana* Asn2 encoding asparagine synthetase is involved in the control of nitrogen assimilation and export during vegetative growth. *Plant Cell Environ* 36, 328–342.
- Gauthier PG, Lamothe M, Mahé A, Molero G, Nogués S, Hodges M, Tcherkez G (2013) Metabolic origin of $\delta^{15}\text{N}$ values in nitrogenous compounds from *Brassica napus* L. leaves. *Plant Cell Environ* 36, 128–137
- Givnish TJ (1990) Leaf mottling: relation to growth form and leaf phenology and possible role as camouflage. *Funct Ecol* 4, 463–474.
- Hu F, Zhu Y, Wu W, Xie Y, Huang J (2015) Leaf variegation of *thylakoid formation 1* is suppressed by mutations of specific sigma factors in *Arabidopsis*. *Plant Physiol*, in press, doi:10.1104/pp.15.00549.
- Kato Y, Miura E, Ido K, Ifuku K, Sakamoto W (2009) The variegated mutants lacking chloroplastic FtsHs are defective in D1 degradation and accumulate reactive oxygen species. *Plant Physiol* 151, 1790–1801.

- Lev-Yadun S (2014) Potential defence from herbivory by ‘dazzle effects’ and ‘trickery coloration’ of leaf variegation. *Biol J Linnean Soc* 111: 692-697.
- Lev-Yadun S (2015) The proposed anti-herbivory roles of white leaf variegation. *Progress in Botany* 76, 241-269.
- Powikrowska M, Khrouchtchova A, Martens HJ, Zygadlo-Nielsen A, Melonek J, Schulz A, Krupinska K, Rodermel S, Jensen PE (2013) SVR4 (suppressor of variegation 4) and SVR4-like: two proteins with a role in proper organization of the chloroplast genetic machinery. *Physiol Plant* 150, 477-492.
- Pringsheim EG, Schwarz W (1933) Das Auftreten weissbunter (panaschierter) Pflanzen in der Natur. *Flora* 28, 111-122.
- Putarjunan A, Rodermel S (2014) *gigantean* suppresses *immutans* variegation by interactions with cytokinin and gibberellin signaling pathways. *Plant Physiol* 166, 2115-2132.
- Rosso D, Bode R, Li W, Krol M, Saccon D, Wang S, Schillaci LA, Rodermel SR, Maxwell DP, Hüner NPA (2009) Photosynthetic redox imbalance governs leaf sectoring in the *Arabidopsis thaliana* variegation mutants *immutans*, *spotty*, *var1* and *var2*. *The Plant Cell* 21, 3473-3492.
- Sawhney SK, Prakash V, Naik MS (1972) Nitrate reductase and nitrite reductase activities in induced chlorophyll mutants of barley. *FEBS Letters* 22, 200–202. doi:10.1016/0014-5793(72)80044-9
- Seltmann H (1955) Comparative physiology of green and albino corn seedlings. *Plant Physiol* 30: 258-263.
- Smith HB (1999) Photosynthetic pigmentation - variegation on a theme. *The Plant Cell* 11, 1–3. doi:10.1105/tpc.11.1.1
- Tcherkez G, Hodges M (2008) How stable isotopes may help to elucidate primary nitrogen metabolism and its interactions with (photo)respiration in C₃ leaves. *J Exp Bot* 59, 1685–1693.
- Tcherkez G, Mauve C, Lamothe M, Le Bras C, Grapin A (2011) The ¹³C/¹²C isotopic signal of day-respired CO₂ in variegated leaves of *Pelargonium × hortorum*. *Plant Cell Environ* 34, 270–283. doi: 10.1111/j.1365-3040.2010.02241.x
- Tcherkez G, Guérard F, Gilard F, Lamothe M, Mauve C, Gout E, Bligny R (2012) Metabolomic characterization of the functional division of nitrogen metabolism in variegated leaves. *Funct Plant Biol* 39, 959–967
- Urbanczyk-Wochniak E, Fernie AR (2005) Metabolic profiling reveals altered nitrogen nutrient regimes have diverse effects on the metabolism of hydroponically-grown tomato (*Solanum lycopersicum*) plants. *J Exp Bot* 56: 309-321.
- Werner RA, Schmidt HL (2002) The in vivo nitrogen isotope discrimination among organic plant compounds. *Phytochemistry* 61, 465-484.
- Yu FEI, Fu A, Aluru M, Park S, Xu Y, Liu H, Rodermel S (2007) Variegation mutants and mechanisms of chloroplast biogenesis. *Plant Cell Environ* 30, 350–365.

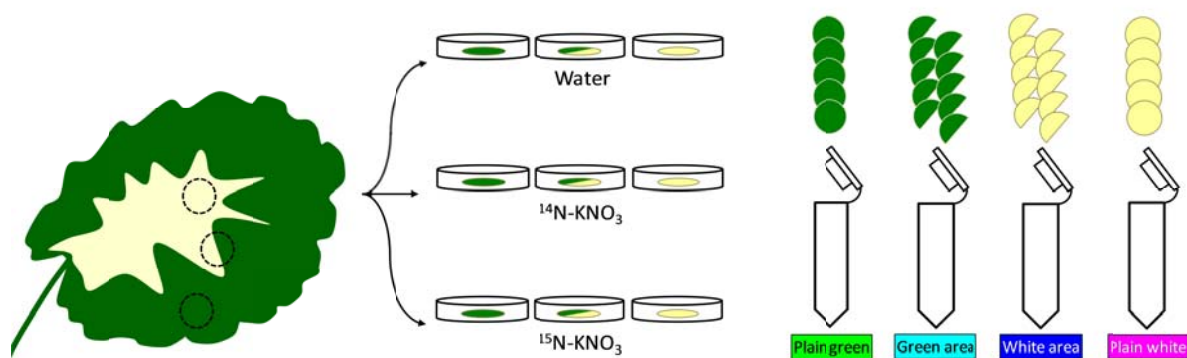


Fig. 1. Schematic of the labelling experiment with leaf discs of *P. × hortorum*. See the text for further details. The color code shown here for sample types is used in Figs. 4 and 5. Samples prepared in this experiment were used for both isotope content in amino acids and metabolomics analyses.

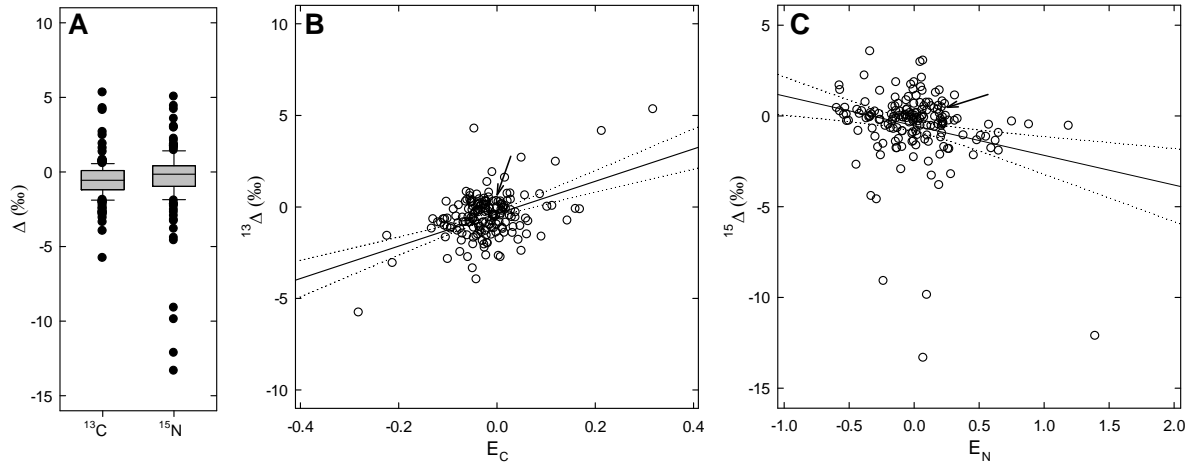


Fig. 2. Isotopic patterns in various variegated plants (sample list in Supplementary Table S1): apparent isotope fractionation between white and green leaf areas (**A**), and relationship between the apparent isotope fractionation (Δ , ‰) and the elemental content offset (E , dimensionless) for carbon (**B**) and nitrogen (**C**). Data associated with *P. × hortorum* are labelled with an arrow. In **A**, fractionation values are not significantly different from 0. In **B** and **C**, linear regression lines (solid) and 95% confidence areas (dotted) are shown. Regressions are $y = -0.36 + 8.85x$ and $R^2 = 0.21$ (significant, $P < 0.05$) **B** and $y = -0.53 - 1.63x$ and $R^2 = 0.06$ (insignificant, **C**).

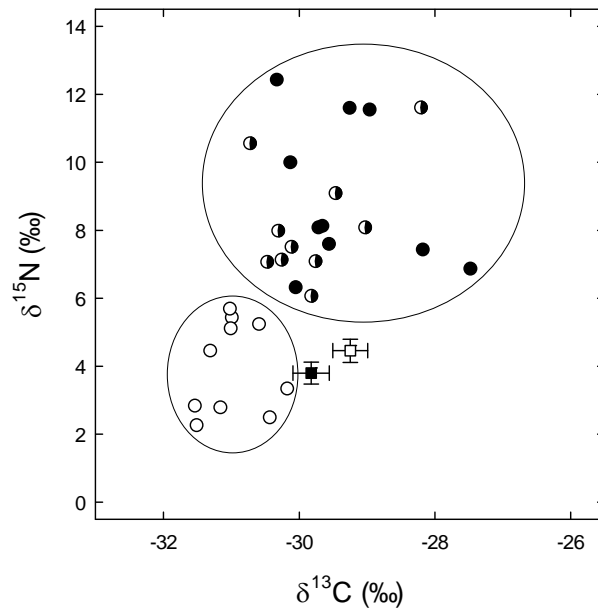


Fig. 3. Natural isotope composition in leaf tissue in *P. × hortorum* under various N-availability conditions: white tissue (open discs) and green tissue (semi-filled) of variegated morphs, and green morphs (closed). Squares represent average \pm SE values for green (closed) and white (open) tissues of various variegated plant species (see Figure 2). Ellipses represent envelope lines to cluster data points.

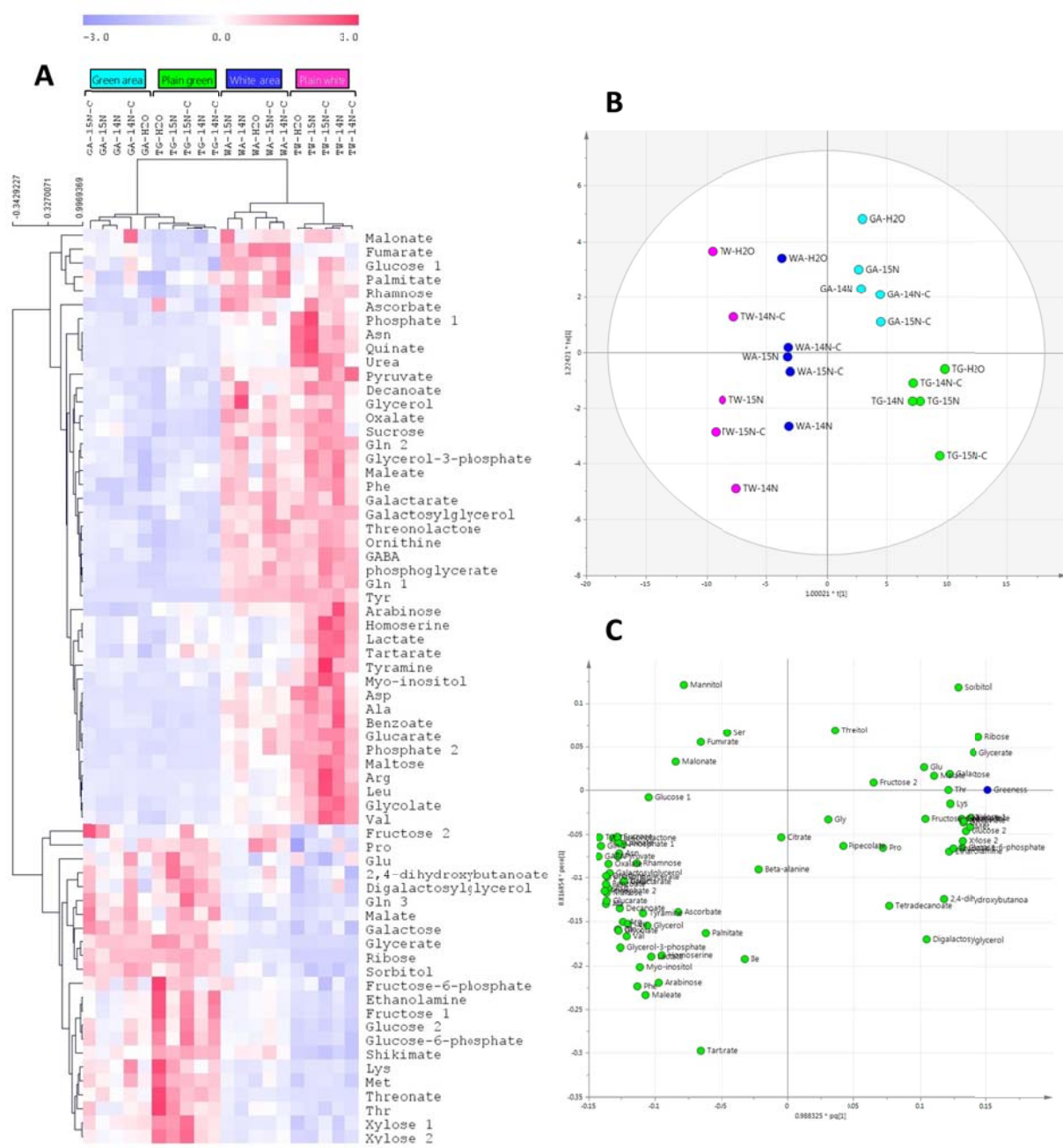


Fig. 4. Metabolomics pattern in white and green leaf discs in the light in *P. × hortorum* under control conditions or with nitrate. **A**, heat map showing metabolites that are significantly different between tissues ($P < 0.05$). A hierarchical clustering (Pearson correlation) is shown on the left for metabolites and on the top for conditions. Each single datum is the average of 5 leaf discs. **B**, OPLS analysis designed to discriminate leaf tissues along a ‘greenness’ scale from plain white leaf discs (left) to plain green discs (right) along axis 1 (x -axis). **C**, loadings of metabolites in the OPLS analysis shown in **B**. A magnified version of this figure is available as Supplementary Fig. S3. Sample types are labelled as follows: TG, plain green leaf discs; GA, green area dissected from variegated leaf discs; WA, white area dissected from variegated leaf discs; plain white leaf discs; ^{15}N or ^{14}N : treated with ^{15}N - or natural nitrate, respectively; H_2O : control discs with distilled water. The symbol ‘C’ refers to a duplicate sampling (6 h).

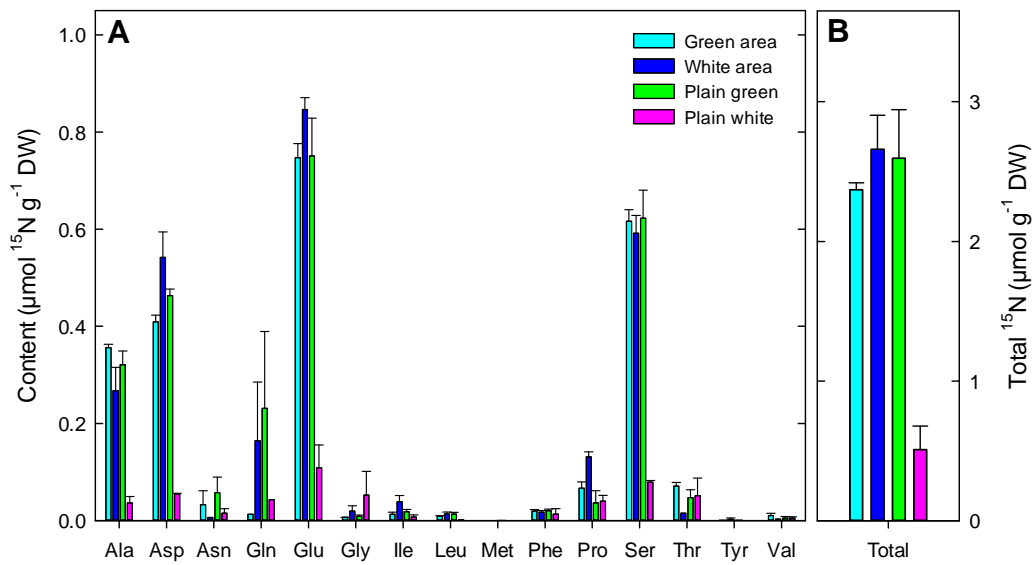


Fig. 5. Incorporation of ^{15}N from $^{15}\text{NO}_3^-$ in illuminated leaf discs of *P. \times hortorum*: individual ^{15}N -amount in amino acid pools determined by GC-MS. Same color legend as in Fig. 4 (also recalled in the legend box).

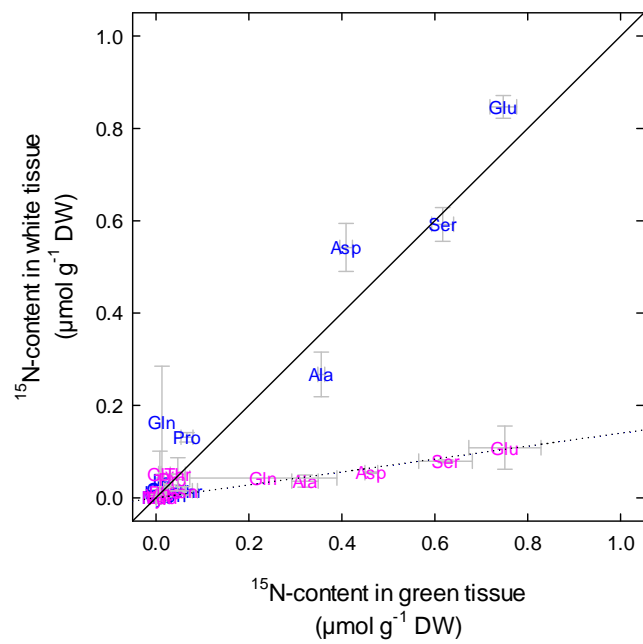


Fig. 6. Comparison of ¹⁵N-amounts in green (x-axis) and white (y-axis) leaf tissue: green vs. white tissues of the same leaf disc (blue), and white vs. green plain tissues (pink). Redrawn from Fig. 5. The continuous line stands for the 1:1 relationship. The dotted line represents a slope of 14%.

Supplemental information

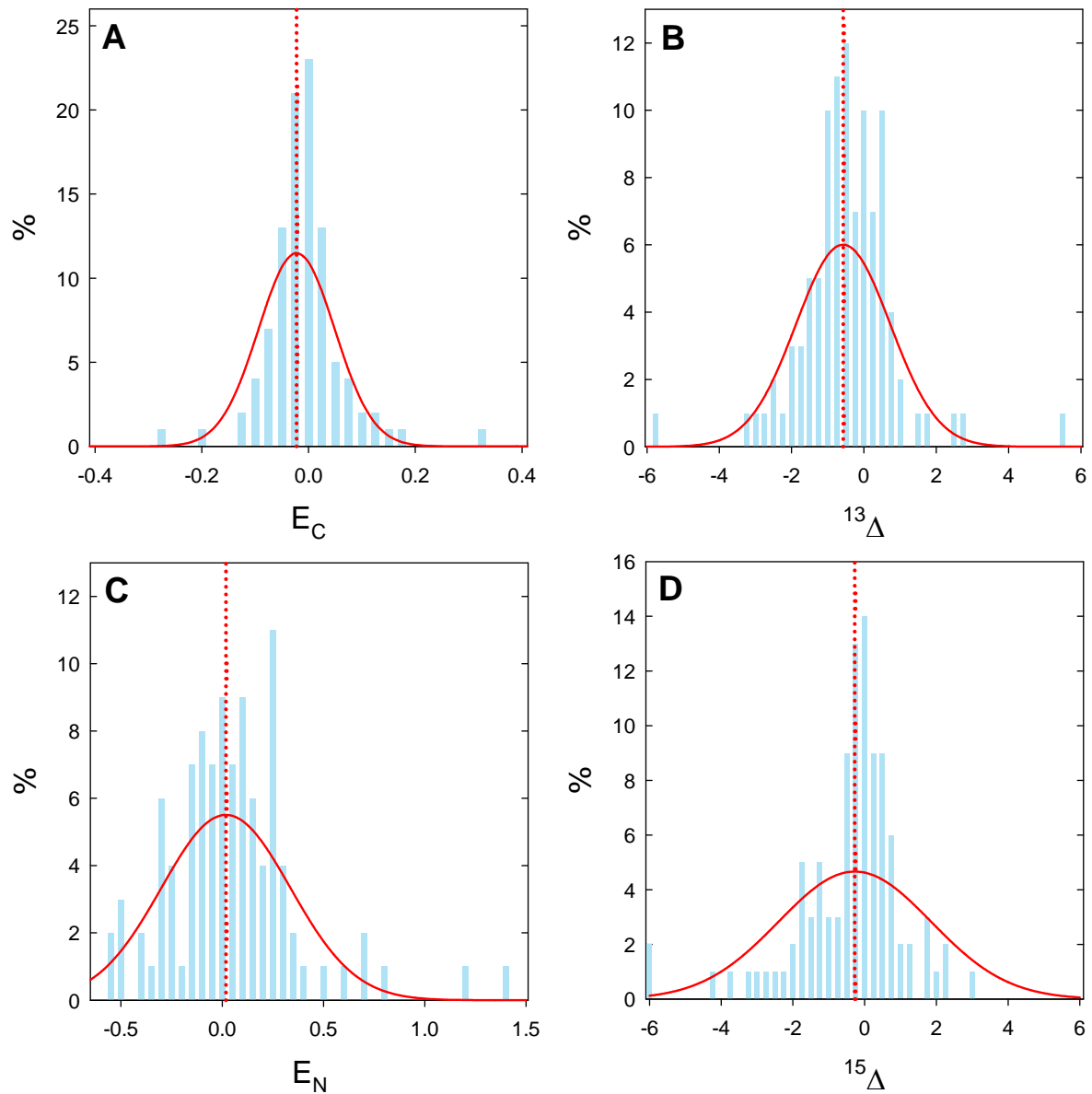


Fig. S1. Frequency distribution of the relative difference in elemental composition (E_C and E_N , **A** and **C**) and apparent isotope fractionation ($^{13}\Delta$ and $^{15}\Delta$, **B** and **D**) between green and white tissues of the same leaf, in different species and locations ($n = 101$).

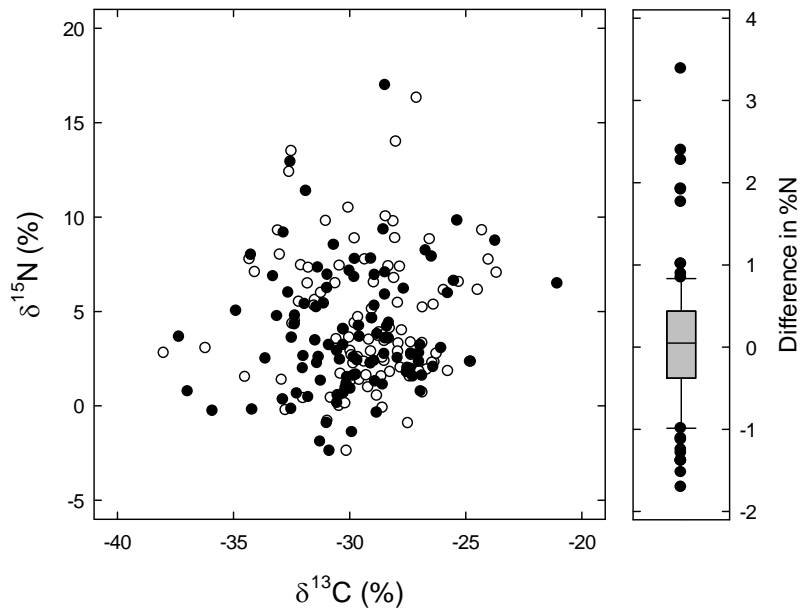


Fig. S2. Comparison of the natural isotope composition in white (open discs) and green (closed discs) tissues of variegated leaves collected in different species. Right, difference in %N between white and green tissues.

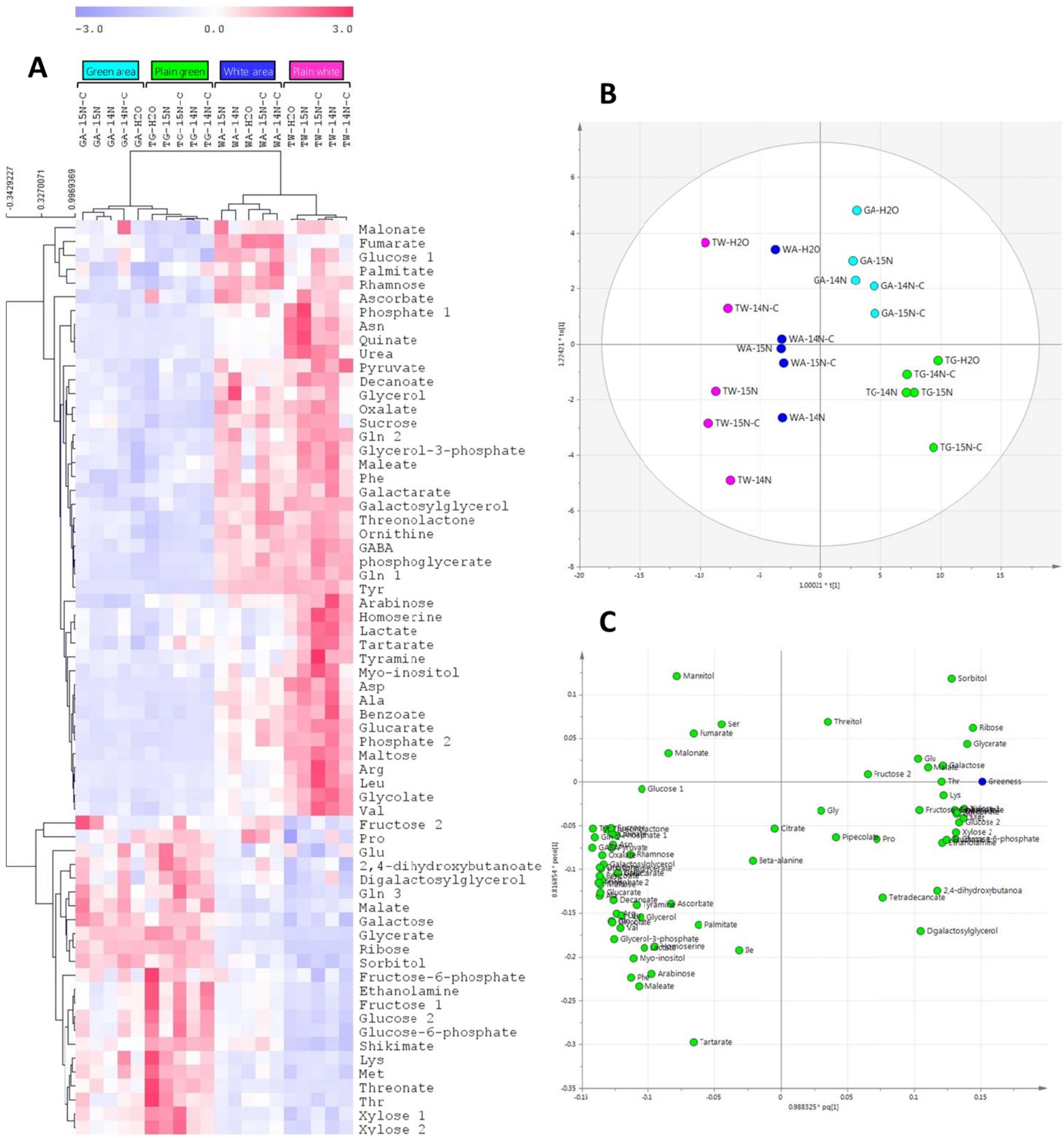


Fig. S3. Magnified version of Fig. 4.

Table S1. List of variegated leaf samples used in this study for elemental and isotopic measurements (Fig. 1).

No.	French Name	Name/Variety	Scientific Name	Family	Order	Collection place	Town	Country	Sampling date DD/MM/YYYY
1	Pothos	Pothos	<i>Epipremnum aureum</i>	Araceae	Alismatales	Greenhouse	Elancourt	France	16/02/2012
2	Cyprès de Lawson	Lawson Cypress	<i>Chamaecyparis lawsoniana</i>	Juniperaceae	Coniferales	Public garden	Elancourt	France	16/02/2012
3	Misère	Rainbow Hill	<i>Tradescantia quadricolor</i>	Commelinaceae	Commelinales	Greenhouse	Elancourt	France	16/02/2012
4	Dieffenbechia	Tropic snow	<i>Dieffenbechia amonea</i>	Araceae	Alismatales	Greenhouse	Elancourt	France	16/02/2012
5	Arbre aux parapluies	Umbrella tree	<i>Shefflera arboricola</i>	Araliaceae	Apiales	Greenhouse	Elancourt	France	16/02/2012
6	Pléoméle	Pleomele	<i>Pleomele reflexa</i>	Asparagaceae	Asparagales	Greenhouse	Elancourt	France	16/02/2012
7	Figuier d'intérieur	Benjamin's fig	<i>Ficus benjamina</i>	Moraceae	Urticales	Greenhouse	Elancourt	France	16/02/2012
8	Fusain	Spindle tree	<i>Euonymus fortunei</i>	Celastraceae	Celastrales	Public garden, La Walk	Wissembourg	France	23/03/2012
9	Fusain	Spindle tree	<i>Euonymus fortunei var. Emerald</i>	Celastraceae	Celastrales	Botanic garden, University Paris-Sud	Orsay	France	19/04/2012
10	Fusain	Spindle tree	<i>Euonymus japonicus var. aureopictus</i>	Celastraceae	Celastrales	Botanic garden, University Paris-Sud	Orsay	France	19/04/2012
11	Cyprès de Lawson	Lawson Cypress	<i>Chamaecyparis lawsoniana</i>	Juniperaceae	Coniferales	Botanic garden, University Paris-Sud	Orsay	France	19/04/2012
12	Croton	Croton Gold Dust	<i>Codiaeum variegatum</i>	Euphorbiaceae	Malpighiales	Garden Les Filaos	Saly	Senegal	26/04/2012
13	Laurier-Rose	Oleander	<i>Nerium oleander</i>	Apocynaceae	Gentianales	Garden Les Filaos	Saly	Senegal	26/04/2012
14	Arbre aux parapluies	Umbrella tree	<i>Shefflera arboricola</i>	Araliaceae	Apiales	Lake Rethba	Niaga Peulh	Senegal	24/04/2012
15	Erable palmé	Maple	<i>Acer palmatum</i>	Aceraceae	Sapindales	Greenhouse of Gally	Versailles	France	1/07/2012
16	Figuier caoutchouc	Elastic fig	<i>Ficus elastica</i>	Moraceae	Urticales	Greenhouse of Gally	Versailles	France	1/07/2012
17	Troène du Japon	Privet	<i>Ligustrum japonicum</i>	Oleaceae	Lamiales	Greenhouse of Gally	Versailles	France	1/07/2012
18	Pépéromia	Radiator plant	<i>Peperomia sp.</i>	Piperaceae	Piperales	Greenhouse of Gally	Versailles	France	1/07/2012
19	Coleus	Coleus	<i>Solenastemon sp.</i>	Lamiaceae	Lamiales	Greenhouse of Gally	Versailles	France	1/07/2012
20	Plectranthus	Plectranthus	<i>Plectranthus coleoides</i>	Lamiaceae	Lamiales	Greenhouse of Gally	Versailles	France	1/07/2012
21	Plectranthus	Plectranthus	<i>Plectranthus coleoides</i>	Lamiaceae	Lamiales	Greenhouse	Elancourt	France	30/05/2012
22	Impatiens de Nouvelle Guinée	Touch me not	<i>Impatiens hawkeri</i>	Balsaminaceae	Ericales	Greenhouse	Elancourt	France	30/05/2012
23	Pittosporum à petites feuilles	Cheesewood	<i>Pittosporum tenuifolium var. variegatum</i>	Pittosporaceae	Apiales	Greenhouse	Elancourt	France	30/05/2012
24	Saule crevette	Japanese willow	<i>Salix integra</i>	Salicaceae	Salicales	Greenhouse	Elancourt	France	30/05/2012
25	Fusain	Spindle tree	<i>Euonymus fortunei</i>	Celastraceae	Celastrales	Greenhouse	Elancourt	France	30/05/2012
26	Troène du Japon	Privet	<i>Ligustrum japonicum</i>	Oleaceae	Lamiales	Greenhouse	Elancourt	France	30/05/2012
27	Unknown	Unknown	<i>Unknown</i>	Unknown	Unknown	Greenhouse	Elancourt	France	30/05/2012
28	Erable négundo	Boxelder maple	<i>Acer negundo</i>	Aceraceae	Sapindales	Greenhouse	Elancourt	France	30/05/2012
29	Cornouiller sanguin	Common dogwood	<i>Cornus sanguineum</i>	Cornaceae	Cornales	Potager du roi	Versailles	France	12/05/2012
30	Peucedan	Peucedanum	<i>Peucedanum ostruthium</i>	Apiaceae	Apiales	Potager du roi	Versailles	France	12/05/2012
31	Weigela	Weigela	<i>Weigela florida var. variegata</i>	Caprifoliaceae	Dipsacales	Potager du roi	Versailles	France	12/05/2012
32	Abutilon	Chinese lantern	<i>Abutilon vitifolium</i>	Malvaceae	Malvales	Potager du roi	Versailles	France	12/05/2012
33	Fusain	Spindle tree	<i>Euonymus fortunei</i>	Celastraceae	Celastrales	Potager du roi	Versailles	France	12/05/2012
34	Géranium citronnelle	Rose geranium	<i>Pelargonium graveolens</i>	Geraniaceae	Geraniales	Potager du roi	Versailles	France	12/05/2012
35	Hosta	Plantain lily	<i>Hosta fortunei var. undulata</i>	Asparagaceae	Asparagales	Public garden	Arcachon	France	28/04/2012
36	Chalef	Silverberry	<i>Eleagnus pungens var. maculata</i>	Eleagnaceae	Rosales	Public garden	Arcachon	France	28/04/2012
37	Pittosporum	Cheesewood	<i>Pittosporum tobira var. variegatum</i>	Pittosporaceae	Apiales	Public garden	Arcachon	France	28/04/2012
38	Pittosporum à petites feuilles	Cheesewood	<i>Pittosporum tenuifolium var. variegatum</i>	Pittosporaceae	Apiales	Public garden	Arcachon	France	28/04/2012
39	Morelle	Nightshade	<i>Solanum jasminoides var. variegatum</i>	Solanaceae	Solanales	Public garden	Elancourt	France	22/07/2012
40	Géranium citronnelle	Rose geranium	<i>Pelargonium graveolens</i>	Geraniaceae	Geraniales	Public garden	Elancourt	France	22/07/2012
41	Chèvrefeuille rampant	Privet honeysuckle	<i>Lonicera pileata</i>	Caprifoliaceae	Dipsacales	Public garden	Elancourt	France	22/07/2012
42	Lierre	Ivy	<i>Hedera helix</i>	Araliaceae	Apiales	Public garden	Arcachon	France	28/04/2012
43	Cornouiller sanguin	Common dogwood	<i>Cornus sanguineum</i>	Cornaceae	Cornales	Public garden	Maurepas	France	22/07/2012
44	Spirée du Japon	Japanese spiraea	<i>Spiraea japonica var. Anthony Waterer</i>	Rosaceae	Rosales	Public garden	Brumath	France	18/08/2012
45	Eulalie	Chinese silver grass	<i>Miscanthus sinensis var. Cabaret</i>	Poaceae	Poales	Lake Chamboux	Peyrelevede	France	31/07/2012
46	Houx	Holly	<i>Ilex aquifolium</i>	Aquifoliaceae		Public garden	Murat	France	15/08/2012
47	Sauge officinale	Sage	<i>Salvia officinalis</i>	Lamiaceae	Lamiales	Greenhouse of Gally	Versailles	France	26/08/2012
48	Lysimaque	Yellow loosestrife	<i>Lysimachia vulgaris</i>	Primulaceae	Primulales	Greenhouse of Gally	Versailles	France	26/08/2012
49	Erable négundo	Boxelder maple	<i>Acer negundo</i>	Aceraceae	Sapindales	Greenhouse	Elancourt	France	24/08/2012

50	Véronique arbustive	Hebe	<i>Hebe franciscana x andersonii</i>	Plantaginaceae	Lamiales	Greenhouse	Elancourt	France	24/08/2012
51	Gaura	Gaura	<i>Gaura chinensis</i>	Onagraceae	Myrtales	Greenhouse	Elancourt	France	24/08/2012
52	Coréopsis	Large-flowered tickseed	<i>Coreopsis grandiflora</i>	Asteraceae	Asterales	Greenhouse	Elancourt	France	24/08/2012
53	Pervenche	Periwinkle	<i>Vinca major</i>	Apocynaceae	Gentianales	Public garden André Citroën	Paris	France	21/08/2012
54	Bambou nain doré	Dwarf golden bamboo	<i>Pleioblastus fortunei var. variegata</i>	Poaceae	Poales	Public garden André Citroën	Paris	France	21/08/2012
55	Laïche japonaise	Japanese sedge	<i>Carex morrowii var. variegata</i>	Cyperaceae	Cyperales	Public garden André Citroën	Paris	France	21/08/2012
56	Vigne-vierge à fruits bleus	Porcelain berry	<i>Ampelopsis brevipedunculata</i>	Vitaceae	Rhamnales	Public garden André Citroën	Paris	France	21/08/2012
57	Iris	Iris	<i>Iris germanica</i>	Iridaceae	Asparagales	Public garden	Elancourt	France	7/10/2012
58	Lierre	Ivy	<i>Hedera helix</i>	Araliaceae	Apiales	Public garden	Elancourt	France	7/10/2012
59	Bugle	Bugle	<i>Ajuga reptans</i>	Lamiaceae	Lamiales	Greenhouse of Maurepas	Maurepas	France	22/09/2012
60	Osmanthus	Chinese osmanthus	<i>Osmanthus heterophyllus var. tricolor</i>	Oleaceae	Lamiales	Greenhouse of Maurepas	Maurepas	France	22/09/2012
61	Phormium	Flax lily	<i>Phormium tenax</i>	Xanthorrhoeaceae	Asparagales	Greenhouse of Maurepas	Maurepas	France	22/09/2012
62	Ciste à feuille de sauge	Rockrose	<i>Cistus salvifolius var. rospico</i>	Cistaceae	Malvales	Greenhouse of Maurepas	Maurepas	France	22/09/2012
63	Abélia	Glossy abelia	<i>Abelia x grandiflora</i>	Caprifoliaceae	Dipsacales	Greenhouse of Maurepas	Maurepas	France	22/09/2012
64	Pieris	Japanese andromeda	<i>Pieris japonica</i>	Ericaceae	Ericales	Greenhouse of Maurepas	Maurepas	France	22/09/2012
65	Euphorbe Hélène	Spurge	<i>Euphorbia milii x lophogona</i>	Euphorbiaceae	Malpighiales	Greenhouse of Maurepas	Maurepas	France	22/09/2012
66	Pépéromia	Radiator plant	<i>Peperomia sp.</i>	Piperaceae	Piperiales	Greenhouse	Elancourt	France	2/12/2012
67	Géranium panaché	Variegated pelargonium	<i>Pelargonium x hortorum</i>	Geraniaceae	Geraniales	Public Town Greenhouse	Elancourt	France	27/04/2013
68	Lierre terrestre	Ground ivy	<i>Glechoma hederacea</i>	Lamiaceae	Lamiales	Public Town Greenhouse	Elancourt	France	27/04/2013
69	Tulipe	Tulip	<i>Tulipa sp.</i>	Liliaceae	Liliales	Greenhouse of Gally	Versailles	France	1/05/2013
70	Laurier-Rose	Oleander	<i>Nerium oleander</i>	Apocynaceae	Gentianales	Public garden	Narrabri	Australia	16/11/2012
71	Millepertuis	Saint John's wort	<i>Hypericum perforatum</i>	Hypericaceae	Theales	Meadow	Burra	Australia	15/11/2012
72	Arbre corail	Coral tree	<i>Erythrina numerosa</i>	Fabaceae	Fabales	Mount Annan Bot. Garden	Cambden	Australia	15/05/2013
73	Syngonium auriculé	Arrowhead vine	<i>Syngonium auritum</i>	Araceae	Alismatales	Public garden	Saint-Pierre	Martinique	15/02/2013
74	Dragonnier	Dragon tree	<i>Dracaena sp.</i>	Asparagaceae	Asparagales	Public garden	Saint-Pierre	Martinique	15/02/2013
75	Feuillage fleur	Breynia	<i>Breynia nivosa</i>	Phyllanthaceae	Malpighiales	Botanic garden	Balata	Martinique	16/02/2013
76	Aglaonema	Dumbcane	<i>Aglaonema pseudobracteatum</i>	Araceae	Alismatales	Botanic garden	Balata	Martinique	16/02/2013
77	Aglaonema	Dumbcane	<i>Aglaonema sp. var. Silver queen</i>	Araceae	Alismatales	Botanic garden	Balata	Martinique	16/02/2013
78	Gazon de Saint Augustin	St Augustine Grass	<i>Stenotaphrum secundatum</i>	Poaceae	Poales	Botanic garden	Balata	Martinique	16/02/2013
79	Manteau de Jacob	Beefsteak plant	<i>Acalypha wilkesiana</i>	Euphorbiaceae	Malpighiales	Public garden	Fort de France	Martinique	17/02/2013
80	Ananas requin	Red pineapple	<i>Ananas bracteatus var. Striatus</i>	Bromeliaceae	Poales	Botanic garden	Balata	Martinique	16/02/2013
81	Hibiscus	Hibiscus	<i>Hibiscus rosa-sinensis</i>	Malvaceae	Malvales	Public garden	Schoelcher	Martinique	18/02/2013
82	Heuchera	Jill of the rocks	<i>Heuchera maxima</i>	Saxifragaceae	Rosales	Public garden	Schoelcher	Martinique	18/02/2013
83	Bougainvillée	Bougainvillea	<i>Bougainvillea spectabilis</i>	Nyctaginaceae	Caryophyllales	Public garden	Le Diamant	Martinique	19/02/2013
84	Croton	Croton Gold Dust	<i>Codiaeum variegatum var. narrow-leaved</i>	Euphorbiaceae	Malpighiales	Public garden	Le Diamant	Martinique	19/02/2013
85	Graptophylle	Caricature plant	<i>Graptophyllum pictum var. tricolor</i>	Acanthaceae	Lamiales	Public garden	Fort de France	Martinique	17/02/2013
86	Croton	Croton Gold Dust	<i>Codiaeum variegatum var. large-leaved</i>	Euphorbiaceae	Malpighiales	Public garden	Fort de France	Martinique	17/02/2013
87	Arbre aux parapluies à grandes feuilles	Large-leaved umbrella tree	<i>Shefflera actinophylla</i>	Araliaceae	Apiales	Public garden	Fort de France	Martinique	17/02/2013
88	Croton	Croton Gold Dust	<i>Codiaeum variegatum var. small-leaved</i>	Euphorbiaceae	Malpighiales	Public garden	Fort de France	Martinique	17/02/2013
89	Marantha	Prayer plant	<i>Calathea ornata</i>	Maranthaceae	Zingiberales	Public garden	Fort de France	Martinique	17/02/2013
90	Ananas requin	Red pineapple	<i>Ananas bracteatus var. Striatus</i>	Bromeliaceae	Poales	Botanic garden	Balata	Martinique	16/02/2013
91	Piléa	Aluminium plant	<i>Pilea cadierei</i>	Urticaceae	Urticales	Botanic garden	Balata	Martinique	16/02/2013
92	Bambou	Bamboo	<i>Bambusa variegata</i>	Poaceae	Poales	Botanic garden	Balata	Martinique	16/02/2013
93	Alpinia	Alpinia	<i>Alpinia sanderae</i>	Zingiberaceae	Zingiberales	Botanic garden	Balata	Martinique	16/02/2013
94	Bambou	Bamboo	<i>Bambusa variegata</i>	Poaceae	Poales	Botanic garden	Balata	Martinique	16/02/2013
95	Liane à barrique	Dalbergia	<i>Dalbergia escataphyllum</i>	Fabaceae	Fabales	Public garden	Saint-Pierre	Martinique	15/02/2013
96	Impatience	Touch-me-not	<i>Impatiens bicornuta</i>	Balsaminaceae	Ericales	Public garden	Fort de France	Martinique	17/02/2013
97	Herbe dure	Mallow	<i>Malvastrum coromandelianum</i>	Malvaceae	Malvales	Parc Anse Couleuvre	Saint-Pierre	Martinique	20/02/2013
98	Arbre aux parapluies	Umbrella tree	<i>Shefflera arboricola</i>	Araliaceae	Apiales	Public garden	Saint-Pierre	Martinique	15/02/2013
99	Dragonnier	Dragon tree	<i>Dracaena sp.</i>	Asparagaceae	Asparagales	Public garden	Saint-Pierre	Martinique	15/02/2013
100	Croton	Croton Gold Dust	<i>Codiaeum variegatum var. narrow-leaved</i>	Euphorbiaceae	Malpighiales	Public garden	Saint-Pierre	Martinique	15/02/2013
101	Micocoulier	Hackberry tree	<i>Celtis occidentalis</i>	Ulmaceae	Urticales	Public garden	Rouen	France	9/08/2013